A semi-automated method for liver tumor segmentation based on 2D region growing with knowledge-based constraints

Damon Wong[1], Jiang Liu[1], Yin Fengshou[1], Qi Tian[1], Wei Xiong[1], Jiayin Zhou[2], Yingyi Qi[2], Thazin Han[2], Sudhakar K Venkatesh[2], and Shih-chang Wang[2]

1. Institute for Infocomm Research, Agency for Science, Technology and Research, Singapore
2. Department of Diganostic Radiology, National University of Singapore, Singapore
3. School of Computing, National University of Singapore, Singapore

Abstract. Liver tumour segmentation from computed tomography (CT) scans is a challenging task. A semi-automatic method based on 2D region growing with knowledge-based constraints is proposed to segment lesions from constituent 2D slices obtained from 3D CT images. Minimal user involvement is required to define an approximate region of interest around the suspected legion area. The seed point and feature vectors are then calculated and voxels are labeled using a region-growing approach. Knowledge-based constraints are incorporated into the method to ensure the size and shape of the segmented region is within acceptable parameters. The individual segmented lesions can then be stacked together to generate a 3D volume. The proposed method was tested on a training set of 10 tumours and a testing set of 10 tumours. To evaluate the results quantitatively, various measures were used to generate scores. Based on the results obtained from the 10 testing tumours, the method was resulted in an average score of 64.

1 Introduction

According to a recent report on cancer statistics[1], liver tumor is the third highest cause of death due to cancer. Although the incidence rate is the sixth highest, at 5.7% of new cancer cases, or 626,000 cases, the mortality rate due to liver cancer is almost as high at 598,000. The high mortality rate has been attributed to poor prognosis of the disease, which underscores the need for an accurate assessment of the cancer.

Computed Tomography (CT) scans are widely used mode of non-destructive and non-invasive imaging for observation of internal physiological structures in the body. The near-isotropic features of modern CT machines allows for volumetric reconstruction obtained via individual slices by stacking the CT slices accordingly. Particularly for diagnosis of liver cancer, it is important to obtain an accurate portrayal of the size of the tumour to determine its severity. Furthermore, tumour localization and volume determination is important for radiotherapeutic treatment management in techniques such as 3D Conformal Radiotherapy (3DCRT) and

Intensity Moduldated Radiotherapy (IMRT), where tumor information is vital for correct dosimetry calculations.

To identify tumours from CT slice images, there is a need for identification, or segmentation, of tumourous lesions. Typically, this has been manually done by trained clinicians. The task is time-consuming, requiring much effort and can be subjective depending on the skill, expertise and experience of the clinician. Objective, computer-aided segmentation of CT images would thus be a great boon for lesion identification. However, this remains a challenging task, due to a number of factors, mainly the low density contrast between lesions and surrounding normal liver tissues, but also, and not limited to, the irregularity of the shape of the lesions and the similarities in image characteristics of the liver with surrounding organs.

A number of methods have been proposed for the computer-aided segmentation of tumours from medical images. In [2], Mahr et al reviewed and compared the various techniques which included region-growing, isocontour, snakes, hierarchical and histogram-based methods, and found that region-growing and snakes, also sometimes known as active contour models, were the most promising for future investigation on liver volumetry determination. In [3], Liu et al reported on the use of a snake algorithm based on gradient vector flow for liver segmentation, incorporating the use of a liver template and edge detection for better initialization of the method. A possible limitation on the use of active contour models is their reliance on a model for initialization to produce an accurate segmentation. In tumour segmentation, the large variability of the shape of lesions for different patients and possibly even for different slices of the same tumour can be a challenge to model.

Seeded region-growing [4] techniques are also another popular method for medical image segmentation[5]. Typically, features are generated from a select number of seed points, and the initial region is gradually increased by incorporating neighbouring pixels with similar feature vectors. The method takes advantage of the potential similarities of pixels belonging to the same structure and can be effective if proper features are chosen. However, the method requires the selection of proper seed points, as incorrect seeds would lead to wrong segmentations. Furthermore, region-growing can be highly computationally-intensive particularly for large images.

Recently, there has also been a trend to utilize *a priori* information into segmentation and classification methods to improve their effectiveness by incorporating heuristics specific to the task. Also known as knowledge-based techniques, these methods make use of domain-knowledge to filter out extraneous regions by employing heuristic-based contraints and filters, or to aid classification through use of templates and landmarks. Knowledge-based techniques have been used to identify abdominal organs [6] and identify brain tumours [7] from CT slices.

In this paper, we propose a semi-automated method to identify tumours from 3D CT scans. After decomposing the 3D scan into its component slices, we apply 2D region growing with knowledge-based constraints on each slice. User interaction is employed to establish an approximate region of interest (ROI) around the lesion in each slice image. This improves the performance of region growing, as well as reduces computational requirements. During the region-growing process, knowledge-based constraints are implemented to constrain the emergent segmented region to within acceptable parameters. In Section 2, an overall framework of the method employed will be presented, followed by a detailed description of the processes used

in the method. Subsequently, in Section 3, we describe the data provided for benchmarking and report on the results obtained on applying our method to the testing data. Section 4 ends the paper with a discussion of the results and conclusion of the findings from the method presented here.

2 Method

For the method presented, we adopted a semi-supervised method based on 2D region growing with knowledge-based constraints to segment the lesions from the CT images. Figure 1 shows the overall framework for the lesion segmentation. The selection of the start and end slices for the segmentation would need to be manually defined, after which the method is applied on each of the selected slices. The following subsections describe the steps employed in greater detail.

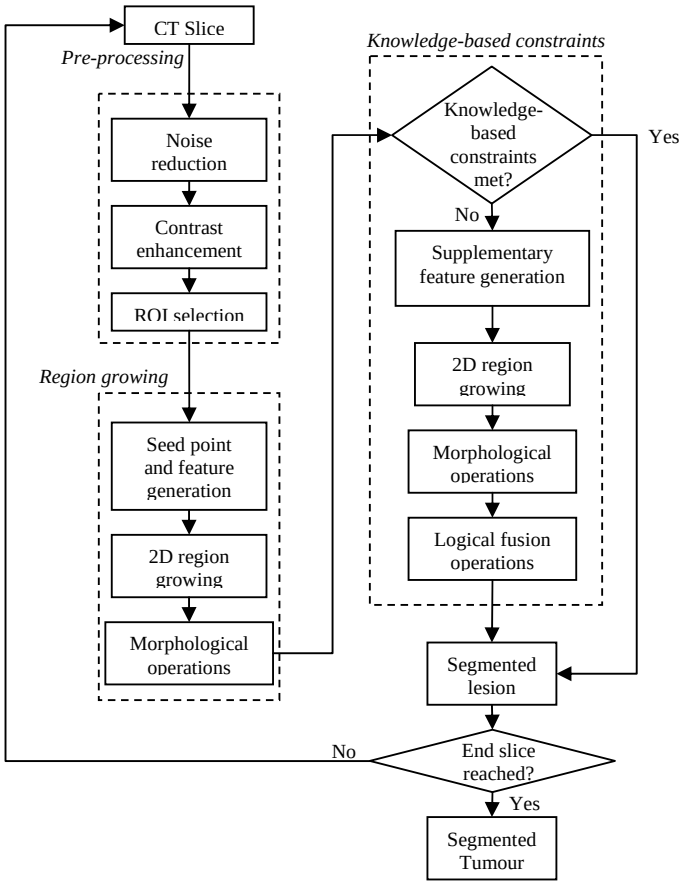

Fig. 1. Liver tumour segmentation process framework.

2.1 Preprocessing, ROI selection and seed point generation

First, to reduce the granular noise in the CT slice image, median filtering via a 3x3 voxel square kernel is convolved across the entire image. Subsequently, the contrast of the CT slice is enhanced to improve visual perception of the structures in the image. Next, a region of interest (ROI) was manually determined by selecting two points on the CT slice image. The two points are used to indicate the diagonal limits of the ROI which contain the tumour lesion. This helps to localize and constrain the region-growing to within the ROI. Furthermore, it helps to avoid inaccurately identifying erroneous regions, particularly outside the liver. ROI selection has to be manually performed only on the first slice. For subsequent slices, the ROI can be reselected, or it can make use of the ROI from the prior slice.

An additional benefit is the reduced processing time by limiting the ROI. For a typical CT slice image with a resolution of 512x512 voxels, generally the size of the lesion is less than 10% of the total number of voxels. Applying the region-growing on only the ROI instead of the entire CT slice would result in savings in the computational requirements.

2.2 Region Growing

Initialization

Next, a seed point for the region growing algorithm is automatically defined at the centre of the ROI. Concurrently, the average voxel intensity in the neighbouring region is calculated and is defined as the initial feature metric. Subsequently, a search is conducted in the 4-connected neighbourhood to determine the voxel which has the least intensity difference from the initial average intensity. The determined voxel is then added to the region.

Iteration

After initialization, the subsequent iterative region-growing process is similar to the method described in [4]**.** Let *L* be the set of voxels labeled as part of the lesion, and *I* be the set of voxels *t* in the ROI which are not part of *L* but are neighbours to *L*. *N(t)* represents the voxels in the immediate neighbourhood of *t*.

$$I = \{t \notin L \mid N(x) \cap L \neq \phi\} \tag{1}$$

Next, the difference in the grayscale intensity levels between the voxels in *I* and the voxels in *L* are calculated as $\delta(t)$.

$$\delta(t) = \left| g(t) - \frac{\sum_{e \in L}^{L} g(e)}{L} \right| \tag{2}$$

The region-growing method then determines the minimum $\delta(t)$

$$t_1 = \min_{t \in I} \delta(t) \tag{3}$$

The voxel t_1 corresponding to the minimum $\delta(t)$ is determined and t_1 is added to the set L. The segmentation labels are updated and the algorithm reiterates until the values of the grayscale intensity in the neighbouring voxels are higher than a pre-defined threshold value, which is empirically obtained. Morphological closing using a flat, disc-shaped structuring element with a voxel radius of 15 is then performed on the segmented region to smoothen out the region boundaries.

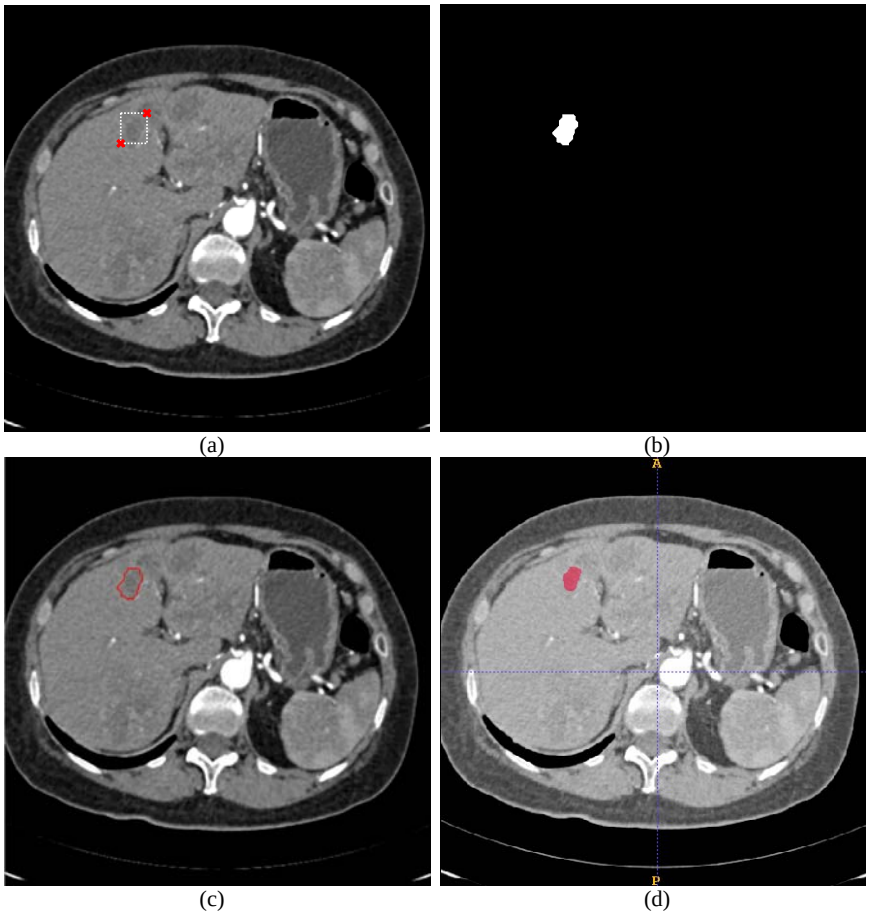

(a) (b) (c) (d)

Fig. 2. Liver tumour segmentation process. (a) shows the manual ROI corner selection. The red crosses indicate the selected points and subsequent ROI is the rectangle with the white dotted outline. The contrast of the CT slice has been enhanced for better differentiation between the various structures. (b) shows the segmented lesion after region-growing and (c) presents the overlay of the boundary from (b) on the original CT slice image, as denoted by the red outline.

(d) shows the ground truth segmentation in red of the lesion. The image is from Slice 139 from Lesion 2 of Patient Data 1.

2.3 Knowledge-based constraints

During the segmentation process, it was found that some attempts resulted in an unusually high regional average intensity, due to the initial seed point being located on bright spots. This caused premature termination of the region-growing algorithm and over-segmentation of the tumour lesion. To avoid these effects, a constraint was imposed on the initial segmented region to occupy a minimum fraction of the total ROI area. The fraction was empirically set but a good approximation was found to be half the size of the ROI. In circumstances where the initially segmented region does not meet this constraint, the region growing is performed again using the same ROI but with a larger area to calculate the initial average intensity. The subsequent segmentation is then fused with the initial segmentation using a logical addition operator, after which morphological closing is applied again to the combined region to obtain the final segmentation result for the CT slice.

3 Testing Data & Results

To evaluate the results using the proposed method, liver tumour CT data sets were provided by the organizers of the workshop. The slices were obtained via a 64-slice and two 40-slice CT scanner in a standard four-in-plane contrast enhanced imaging protocol with a slice thickness of 1mm of 1.5mm, and an in-plane resolution of 0.6-0.9mm. 10 liver tumours from four patients were used for training, and another 10 tumours from five patients were used in testing. A final ten images will be used for the onsite during the segmentation workshop. The datasets represent a range of patients, pathology and CT scanning phases. All the ground truths were manually segmented by an experienced radiologist and confirmed by another radiologist as reference for evaluation purposes.

Figure 3 and 4 show the visual examples of the segmentation results for the training set and the testing set respectively. For Figure 3, the corresponding ground truth results as determined by the radiologists are also included for comparison. The results were also evaluated quantitatively using the following five measures, (1) relatively absolute volume differences, (2) average symmetric absolute surface distance, (3) symmetric RMS surface distance, (4) maximum symmetric absolute surface distance, and (5) volumetric overlap error, and are tabulated in Tables 1 and 2 for the training set and the testing set respectively. For the testing set, an automatic scoring system [7] was used to assign scores to the results obtained under the five measures, with the score ranging from 0 to 100. A score of 100 represents the perfect segmentation while 0 is the minimum score one segmentation will get. Table 2 includes the corresponding scores for the measures.

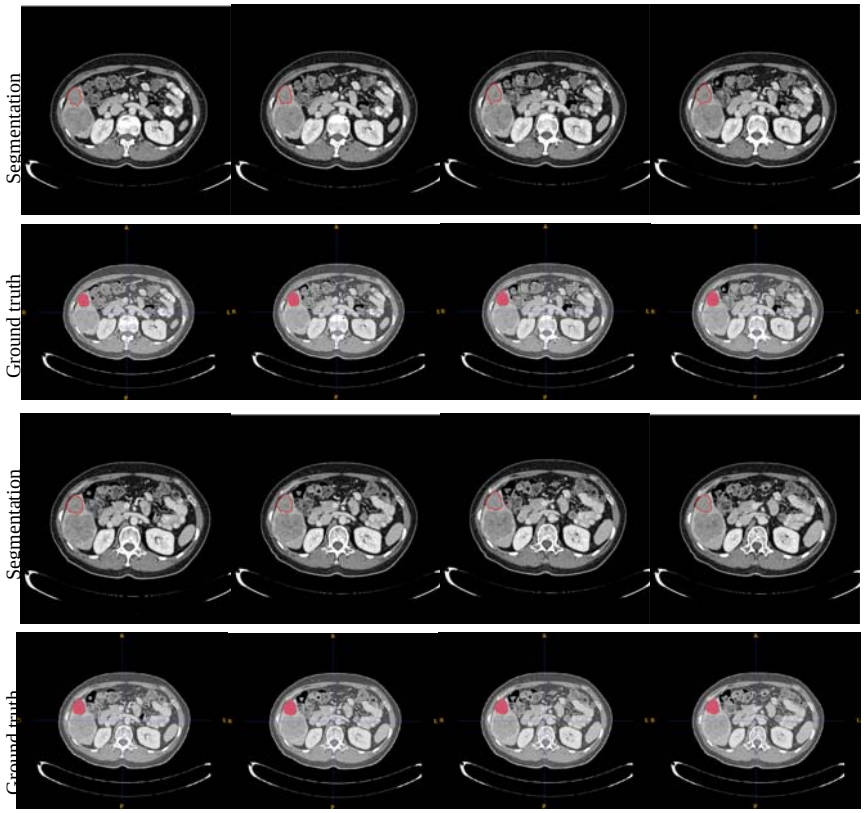

Fig 3. Segmentation results (top row) and ground truth (bottow rom) for Slices 86-93 of Lesion 2 from Dataset 4.

Table 1. Quantitative results obtained from the training data set

Tumor	Overlap Error [%]	Volume difference [%]	Ave. Surf. Dist. [mm]	RMS Surf. Dist. [mm]	Max. Surf. Dist. [mm]
IMG01_L1	34.45	11.2544	2.0702	2.832	14.2655
IMG01_L2	28.7	8.86	1.0226	1.6305	9.8152
IMG02_L1	25.07	3.8759	0.8661	1.3366	9.5636
IMG02_L2	28.61	25.568	1.1983	1.8093	9.3226
IMG02_L3	27.97	7.4968	1.0106	1.5866	8.8689
IMG03_L1	41.99	21.0929	1.0384	1.6694	9.4826
IMG04_L1	18.87	0.891	1.505	2.319	18.3036
IMG04_L2	9.29	2.8418	0.3457	0.6532	5.133
IMG04_L3	11.82	3.1932	0.9703	2.1005	17.7573
IMG04_L4	20.84	12.5498	1.2445	2.0322	11.0206

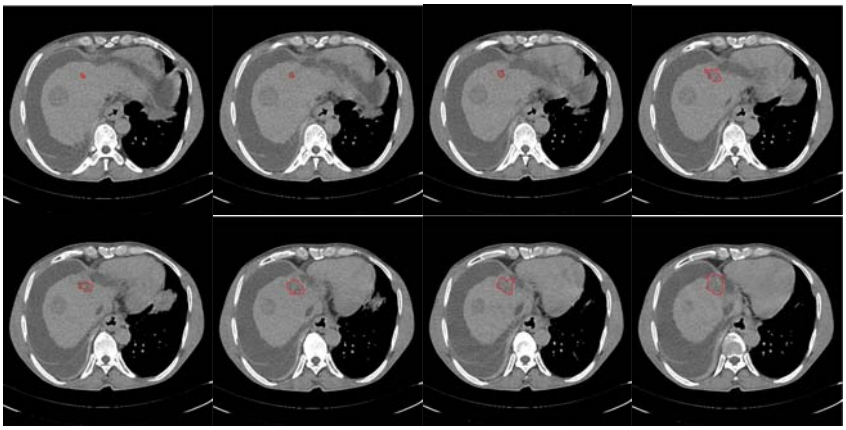

Fig 4. Segmentation results for Slices 163 to 170 of Lesion 3 from Patient Dataset 5.

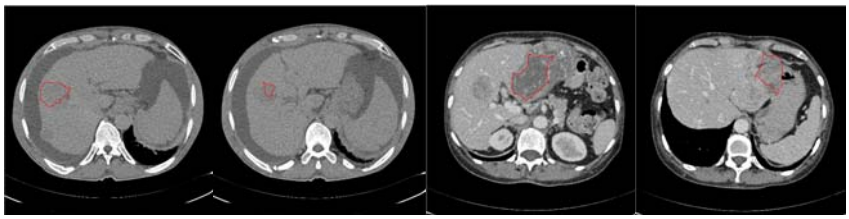

(a) (b) (c) (d)

Fig 5. Selected poor segmentation results from (a) Dataset 5 Slice 143, (b) Dataset 5 Slice 149, (c) Dataset 7 Slice 88 and (d) Dataset 7 Slice 119. The poor segmentation can be attributed to low contrast visibility in (a) and (b), and non-uniform lesion texture in (c) and (d).

Table 2. Quantitative results obtained from the testing data set

	Overlap Error		Volume Difference		Ave. Surf. Dist.		RMS Surf. Dist.		Max. Surf. Dist.		
Tumor	(%)	Score	(%)	Score	(mm)	Score	(mm)	Score	(mm)	Score	Total Score
IMG05_L1	36.05	72	6.78	93	2.99	24	4.17	42	18.59	53	57
IMG05_L2	41.85	68	23.52	76	1.73	56	2.53	65	12.48	69	67
IMG05_L3	36.93	71	3.61	96	1.50	62	2.18	70	10.97	73	74
IMG06_L1	50.06	61	41.81	57	1.20	70	1.61	78	5.23	87	70
IMG06_L2	48.25	63	19.74	80	1.22	69	1.78	75	9.35	77	73
IMG07_L1	40.76	69	35.73	63	5.61	0	7.59	0	29.87	25	31
IMG07_L2	31.46	76	18.87	80	1.60	60	2.25	69	10.18	75	72
IMG08_L1	18.24	86	12.18	87	2.16	45	3.11	57	13.62	66	68
IMG09_L1	46.85	64	38.49	60	1.53	61	2.08	71	7.55	81	67
IMG10_L1	43.50	66	41.22	57	2.45	38	2.95	59	9.07	77	60
Average	39.40	70	24.20	75	2.20	49	3.02	59	12.69	68	64

4 Discussion & Conclusions

From an analysis of the results, the proposed method performs well for lesions that are well-defined and have uniform grayscale intensity throughout the lesion. Although some user interaction is required, the effort needed is minimal as the user need only to define an approximate ROI around the suspected lesion, rather than manually delineating the lesion boundary. Furthermore, the method, combined together with ROI constraints, is relatively fast, with each slice taking about one to two seconds to process in a MATLAB operating environment running on a 3GHz Dual Core Pentium PC with 4 GB RAM. Providing some allowance for adjusting of the parameters, segmenting an entire tumour typically consisting of approximately 25 slices should take about ten minutes.

However, it was observed that for lesions with certain characteristics, segmentation performance was sub-optimal. In particular, for lesions with low contrast compared t0 normal liver tissue, such as in Figs 5(a) and 5(b), the feature space separation between lesion voxels and normal tissue voxels can be minimal, leading to difficulty in accurately labeling voxels. Furthermore, when the lesion has a patchy, non-uniform appearance, as can be seen in Figs 5(c) and 5(d), the visual characteristics of the lesion can be observed to vary even on the same CT slice, since the resultant labeling of voxels would depend on the initial seed selection. Where parts of the lesion have characteristics which are too different from the seed points, these voxels would be mistakenly mis-labelled as non-tumour voxels. Possible strategies to overcome these challenges could be the selection of different features, or aggregating feature vectors from multiple seed regions to increase the robustness of the system.

In this paper, we have presented a semi-automated method for 3D segmentation of tumours from CT slices. First, the 3D scans are decomposed into its constituent parts, after which 2D region-growing with knowledge-based constraints is applied to segment the lesion voxels from the normal tissue voxels. From the results obtained using the training data set and the testing data set, the method was found to perform adequately. Further improvements can be implemented to improve the performance of the proposed method.

Acknowledgements

This work is supported by a research grant (SBIC RP C-008/2006) from the Singapore BioImaging Consortium, Agency for Science, Technology and Research.

References

1. Parkin, D.M., Bray, F, Ferlay, J, Pisani, P.: Global Cancer Statistics 2002.CA Cancer J Clin, 55:74-108 (2005).
2. Mahr, A., Levegrün, S, Bahner, M.L., Kress, J., Zuna, J., Schlegel W.: Usability of semiautomatic segmentation algorithm for tumor volume determination. Invest. Radiol. 34, 143--150 (1999).

3. Liu, F., Zhao, B., Kijewski, P.K., Wang, L., Schwartz, L.H.: Liver segmentation for CT images using GVF snake. Med. Phys. vol. 32(12), 3699-3706, 2005.
4. Adams, R. Bischof, L.: Seeded Region Growing. IEEE Trans. Pattern Anal. Mach. Intell. vol 16(6), pp. 641-647 (1994).
5. Pohle,R., Toennies, K.D.: Segmentation of Medical Images Using Adaptive Region Growing. *Proc. SPIE Medical Imaging*, vol. 4322, pp. 1337–1346. (2001)
6. Kobashi,M. and Shapiro,L.G.: Knowledge-based organ identification from CT images. *Pattern Recogn.*, vol. 28, pp. 475–491 (1995).
7. Clark, M.C. Hall, L.O. Goldgof, D.B. Velthuizen, R. Murtagh, F.R. Silbiger, M.S.: Automatic tumor segmentation using knowledge-based techniques. IEEE Trans. Med. Imaging. vol. 17(2), pp. 187-201 (1998).